Cellular/Molecular

Climbing Fiber-Mediated Spillover Transmission to Interneurons Is Regulated by EAAT4

Shreya Malhotra,[1] Gokulakrishna Banumurthy,[1*] Reagan L. Pennock,[1*] Jada H. Vaden,[1*] ⊕Izumi Sugihara,[2] Linda Overstreet-Wadiche,[1] and Jacques I. Wadiche[1]

[1]Department of Neurobiology and McKnight Brain Institute, University of Alabama at Birmingham, Birmingham, Alabama 35294, and [2]Department of Systems Neurophysiology, Tokyo Medical and Dental University Graduate School of Medical and Dental Sciences, Tokyo, 113-8519, Japan

Neurotransmitter spillover is a form of communication not readily predicted by anatomic structure. In the cerebellum, glutamate spillover from climbing fibers recruits molecular layer interneurons in the absence of conventional synaptic connections. Spillover-mediated signaling is typically limited by transporters that bind and reuptake glutamate. Here, we show that patterned expression of the excitatory amino acid transporter 4 (EAAT4) in Purkinje cells regulates glutamate spillover to molecular layer interneurons. Using male and female Aldolase C-Venus knock-in mice to visualize zebrin microzones, we find larger climbing fiber-evoked spillover EPSCs in regions with low levels of EAAT4 compared with regions with high EAAT4. This difference is not explained by presynaptic glutamate release properties or postsynaptic receptor density but rather by differences in the glutamate concentration reaching receptors on interneurons. Inhibiting glutamate transport normalizes the differences between microzones, suggesting that heterogeneity in EAAT4 expression is a primary determinant of differential spillover. These results show that neuronal glutamate transporters limit extrasynaptic transmission in a non–cell-autonomous manner and provide new insight into the functional specialization of cerebellar microzones.

Key words: cerebellum; EAAT; glutamate; spillover; synaptic transmission

Significance Statement

Excitatory amino acid transporters (EAATs) help maintain the fidelity and independence of point-to-point synaptic transmission. Whereas glial transporters are critical to maintain low ambient levels of extracellular glutamate to prevent excitotoxicity, neuronal transporters have more subtle roles in shaping excitatory synaptic transmission. Here we show that the patterned expression of neuronal EAAT4 in cerebellar microzones controls glutamate spillover from cerebellar climbing fibers to nearby interneurons. These results contribute to fundamental understanding of neuronal transporter functions and specialization of cerebellar microzones.

Introduction

Neuronal circuitry can be established through anatomic analysis of synapses, the sites of direct communication between neurons. However, anatomy cannot predict spillover transmission, in which neurotransmitters escape from the synaptic cleft and activate receptors on neighboring cells or synapses (Asztely et al., 1997; Kullmann, 2000). This type of extrasynaptic communication occurs throughout the brain where it augments canonical point-to-point synaptic transmission by recruiting extrasynaptic receptor activation (Scanziani et al., 1996; Asztely et al., 1997; Isaacson, 1999; Scanziani, 2000; Chalifoux and Carter, 2011; Henneberger et al., 2020). Spillover signaling is prominent in the cerebellum where it occurs in the absence of conventional anatomically defined synapses (Nishiyama and Linden, 2007; Szapiro and Barbour, 2007; Mathews et al., 2012; Coddington et al., 2014; Nietz et al., 2017). While these anatomically independent circuit motifs are engaged during sensory processing and contribute to cerebellar computations (Jörntell and Ekerot, 2002; Arlt and Hausser, 2020), the factors controlling its reach and regulation are not fully understood.

Cerebellar climbing fibers (CFs) form powerful synapses with Purkinje cells (PCs) comprised of hundreds of individual synaptic contacts (Palay and Chan-Palay, 1974). Although individual

synaptic contacts are nearly completely ensheathed by Bergmann glia that express glutamate transporters excitatory amino acid transporters 1 (EAAT1) and 2 (EAAT2) (Rothstein et al., 1994; Tanaka et al., 1997; Xu-Friedman et al., 2001; Huang and Bergles, 2004; Tsukada et al., 2005; Tsai et al., 2012), glutamate can escape the CF-PC synapse to activate receptors on molecular layer interneurons (MLIs) (Kollo et al., 2006; Szapiro and Barbour, 2007; Mathews et al., 2012; Coddington et al., 2013). One molecular mechanism that may regulate the extent of CF-mediated spillover is the expression levels of EAAT4, a high-affinity glutamate transporter located on PCs (Dehnes et al., 1998; Brasnjo and Otis, 2004; Takayasu et al., 2004, 2005). The expression of EAAT4 follows a parasagittal banding pattern similar to the expression of aldolase C (zebrin), creating microzones of molecularly diverse PCs with high and low levels of EAAT4 (Dehnes et al., 1998; Wadiche and Jahr, 2005; Tsai et al., 2012). In contrast, Dehnes et al. (1998) showed that GLAST, GLT, and EAAC (EAAT1-3, respectively) are uniformly expressed throughout the cerebellum. Although glial EAAT1 and EAAT2 are responsible for the reuptake of the majority of glutamate released at the CF-PC synapse, the perisynaptic location of EAAT4 positions it to fine-tune spillover in a synapse-specific manner (Tanaka et al., 1997; Dehnes et al., 1998). We previously showed that patterned expression of EAAT4 mediates differences in parallel fiber (PF)-mediated activation of PC mGluRs as well as extrasynaptic glutamatergic transmission to adjacent Bergmann glia (Wadiche and Jahr, 2005; Tsai et al., 2012). It is not known, however, whether this physiological difference in transporter expression is sufficient to exert a non–cell-autonomous regulation of glutamatergic signaling from CFs to MLIs.

To test whether patterned expression of EAAT4 controls the amount of glutamate spillover reaching MLIs, we use mice expressing Venus under the *Zebrin II/Aldolase C* promoter to compare CF-mediated spillover in high and low EAAT4 microzones (Fujita et al., 2014). We assay postsynaptic NMDAR and AMPAR activation in MLIs and use AMPAR low-affinity antagonists to measure the relative differences in glutamate concentration. We conclude that endogenous differences in EAAT4 expression are sufficient to regulate the extent of spillover transmission onto neighboring MLIs despite glial ensheathment of CF synapses (Xu-Friedman et al., 2001) and differential glutamate release between zebrin microzones (Paukert et al., 2010). These results highlight the functional significance of high-affinity neuronal transporters that appear to provide privileged control of synaptically released glutamate beyond the physical and transporter barriers provided by glia (Tzingounis and Wadiche, 2007; Scimemi et al., 2009).

Materials and Methods
Experimental model and subject details
We used male and female knock-in mice with the GFP Venus inserted into exon 2 of the *Aldolase C* gene on C57BL/6N background (Aldoc-Venus mice) (Fujita et al., 2014). Homozygous mice were maintained in a 12:12 h light:dark cycle and used between postnatal days 12 and 25. Some functional alterations resulting from diminished expression of aldolase C cannot be ignored in experiments using Aldoc-Venus mice. However, several reasons suggest that such alterations may not be significant. First, the expression of aldolase C only starts at postnatal stages (after P9-P14) in PCs (Fujita et al., 2014), around the time of the recordings. Second, the gross shape and size of the brain are indistinguishable among the WT, heterozygote, and homozygote of Aldoc-Venus mice (Fujita et al., 2014). Third, the zebrin pattern is the same among the WT, heterozygote, and homozygote of Aldoc-Venus mice (Fujita et al., 2014). Fourth, general motor performance examined by the rotarod test

showed no significance differences among the WT, heterozygote, and homozygote of Aldoc-Venus mice (Luo et al., 2020). All experiments were conducted through protocols approved by the Institutional Animal Care and Use Committee of the University of Alabama at Birmingham under protocol IACUC-08767.

Slice preparation
Mice were decapitated under isoflurane (VetOne), and the cerebellum was rapidly dissected into ice-cold cutting solution containing the following (in mM): 110 choline chloride, 2.5 KCl, 1.25 NaH_2PO_4, 25 $NaHCO_3$, 25 glucose, 11.5 sodium ascorbate, 3 sodium pyruvate, 0.5 $CaCl_2$, and 7.0 $MgCl_2$, bubbled with 95% O_2, 5% CO_2. The cerebellum was placed in a parasagittal orientation on an agar block, and sections from the vermis (300 μM) were taken using a vibratome (VT1200S, Leica Instruments). Slices were transferred to 35°C ACSF for 30 min and then stored at room temperature for another 30 min. The ACSF contained the following (in mM): 125 NaCl, 2.5 KCl, 1.0 NaH_2PO_4, 26.2 $NaHCO_3$, 11 glucose, 2.5 $CaCl_2$, and 1.3 $MgCl_2$.

Electrophysiology
Recordings were made from slices maintained at ~32°C using an inline heater (ALA Scientific Instruments) with constant flow of ACSF at ~3 ml/min. A 60× water immersion objective on an upright microscope (Olympus) was used to identify PCs and MLIs that were voltage-clamped using a Multiclamp 700B amplifier controlled by pClamp 10.6 software (Molecular Devices). Currents were filtered at 2-5 kHz and digitized at 15-50 kHz using a Digidata 1440A AD converter (Molecular Devices). Patch pipettes were pulled using a P-97 horizontal puller (Sutter Instruments). ACSF contained 100 μM picrotoxin to block $GABA_A$ receptors (Abcam).

MLI recordings. Single CFs were stimulated near the PC layer using a theta glass pipette (Sutter Instruments) filled with bath solution. MLIs in the inner and middle thirds of the molecular layer were patched using thick-wall glass pipettes pulled to a resistance of 2.5-5 MΩ. The position and intensity of the stimulating pipette were adjusted until a single CF (all-or-none response) was detected and PF responses were absent.

Only MLIs and PCs with a single CF were included in our analysis. The pipette solution contained the following (in mM): 100 $CsMeSO_3$, 50 CsCl, 10 HEPES, 10 EGTA, 1 $MgCl_2$, 2 MgATP, 0.3 NaGTP, and 5 QX-314, adjusted to pH 7.2 with CsOH. Cells were held at −60 mV unless otherwise noted, and series resistance (R_s) was measured by the instantaneous current response to a −5 mV step. R_s values were 15–20 MΩ. R_s was uncompensated and monitored throughout recordings.

PC recordings. Patch pipettes were pulled from thin-wall borosilicate glass (Sutter Instruments) to a resistance of 0.8-2.0 MΩ and filled with solution containing the following (in mM): 110 CsCl, 35 CsF, 10 HEPES, 10 EGTA, and 5 QX-314 adjusted to pH 7.2 with CsOH. R_s, measured by the instantaneous current response to a −2 mV step with only pipette capacitance canceled, was <5 MΩ and was routinely compensated >80%. Resistance was monitored throughout the recording, and experiments were discarded if substantial changes were observed (>20%). CFs were stimulated with theta glass electrodes (BT-150, Sutter Instruments) filled with 5% NaCl driven by a constant current isolated stimulator (Digitimer North America) and placed in the granule cell layer.

Drug treatments
Drug concentrations are listed in the text or figure legends. Picrotoxin (GABAAR antagonist), NBQX (AMPAR antagonist), QX-314 (Na^+-channel blocker), (R)-CPP (NMDA antagonist), and kynurenic acid (KYN, low-affinity antagonist) were purchased from Abcam. DL-TBOA (excitatory-amino-acid-transporter blocker) was purchased from HelloBio.

Quantification and statistical analysis
AxoGraph X (Axograph Scientific) and GraphPad Prism (GraphPad) were used for data analysis. Reported values are ± SEM, and the statistical tests used are stated in the figure legends. Means were compared using paired or unpaired two-tailed *t* tests or one- or two-way ANOVAs with Holm-Sidak correction for multiple comparison tests. Extra sum-of-squares *F* tests were used to compare curves fit to different groups
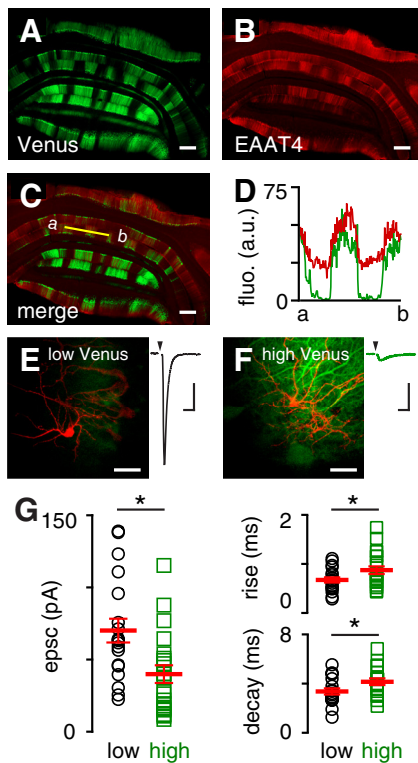
Figure 1. MLIs in low EAAT4 regions have larger spillover responses. *A*, An example of a coronal section from a mouse expressing Venus under the Aldolase C promoter. *B*, EAAT4 antibody staining in the same coronal section. *C*, Overlay of Venus fluorescence and EAAT4 staining. Orientation: dorsal (top) to ventral (down). Scale bars, 200 μm. *D*, Intensity comparison from Venus and EAAT4 antibody staining ($r = 0.81 \pm 0.04$; similar results from $n = 6$ regions of 3 sections). *E*, Representative two-photon imaging of a filled interneuron (red) in low Venus region and corresponding CF-mediated EPSC. *F*, Similar to *E*, a high Venus region. Scale bar, 30 μm. Calibration: 20 pA, 10 ms. *G*, Left, EPSC amplitude (low, black circles: 70.1 ± 8.2 pA, $n = 19$; high, green squares: 39.9 ± 6.1 pA, $n = 21$; $p = 0.005$; unpaired *t* test) and charge (low: 323.1 ± 46.1 fC, $n = 19$; high: 197.8 ± 25.0 fC, $n = 20$; $p = 0.02$; unpaired *t* test; not shown) were significantly smaller in high Venus regions. Right, EPSC rise times (20%-80%; low: 0.67 ± 0.05 ms, $n = 19$; high: 0.87 ± 0.08 ms, $n = 21$; $p = 0.046$; unpaired *t* test) and decay time constants (low: 3.4 ± 0.3 ms, $n = 19$; high: 4.2 ± 0.3 ms, $n = 19$; $p = 0.04$; unpaired *t* test) were slower in high Venus regions.

within the same experiment. The criterion for statistical significance was $p < 0.05$, noted by asterisk (*) in figure and exact p-value in text and legend.

Results

Aldolase C Venus fluorescence correlates with EAAT4 expression

We first confirmed that cerebellar microzones defined by zebrin expression exhibit differential EAAT4 expression. We used mice with the GFP Venus inserted into exon 2 of the Aldolase C gene to visualize the well-known zebrin banding pattern (Aldoc-Venus mice) (Fujita et al., 2014), and compared Venus with the pattern of EAAT4 immunostaining (Fig. 1A–C). We found that Venus and EAAT4 expression were correlated ($r = 0.81 \pm 0.04$; $n = 6$ regions from 3 sections; Fig. 1D), indicating that Venus fluorescence is a good proxy for EAAT4 expression.

Glutamate spillover differs between low and high EAAT4 regions

Although CF-PC synapses are nearly completely ensheathed by Bergmann glia (Xu-Friedman et al., 2001), glutamate receptors
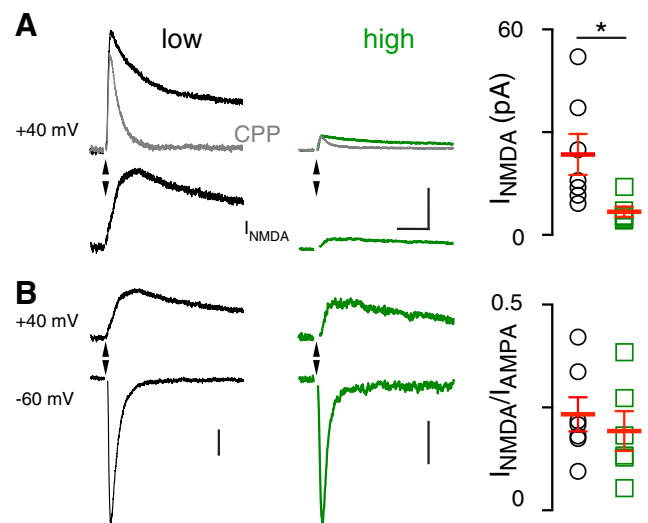

Figure 2. Lower spillover-mediated NMDAR activation in high EAAT4 regions. *A*, Left, CF-mediated EPSCs at 40 mV before and after R-CPP (5 μM, gray) and NMDAR-mediated currents (bottom) obtained by subtracting these two traces in low (left) and high (middle) EAAT4 regions. Right, Summary showing that NMDAR EPSCs are larger in low EAAT4 regions. (Low: 29.1 ± 6.7 pA, $n = 6$; high: 5.6 ± 0.7 pA, $n = 5$; $p = 0.01$; unpaired *t* test). Scale bars, 20 pA, 40 ms. *B*, NMDAR and AMPAR responses at 40 and -60 mV, respectively, in low (left) and high (middle) EAAT4 regions. Right, Lack of difference in the NMDA/AMPA ratio between the high and low EAAT4 regions (low: $n = 7$; high: $n = 6$; $p > 0.05$; unpaired *t* test). Scale bars, 20 pA (left), 5 pA (right).

on neighboring MLIs are activated following CF stimulation despite no anatomic connection (Jörntell and Ekerot, 2003; Szapiro and Barbour, 2007; Mathews et al., 2012; Coddington et al., 2013). This is likely because of multivesicular release at CF to PC synapses that results in a high synaptic glutamate concentration of ∼10 mM at each release site (Wadiche and Jahr, 2001; Rudolph et al., 2011; Vaden et al., 2019). Guided by Venus fluorescence, we recorded CF-evoked spillover EPSCs in MLIs from low and high EAAT4 microzones (Fig. 1E,F). In the presence of picrotoxin (GABA$_A$R antagonist) and R-CPP (NMDAR antagonist), we adjusted the stimulus intensity to evoke an all-or-none CF EPSC without PF contamination using multiple criteria, including the following: (1) all-or-none recruitment, (2) paired-pulse depression, and (3) slow rise and decay times (Coddington et al., 2013; Nietz et al., 2017). AMPAR-mediated CF EPSCs were larger in low EAAT4 regions, measured either by peak amplitude (low, black circles: 70.1 ± 8.2 pA, $n = 19$; high, green squares: 39.9 ± 6.1 pA, $n = 21$; $p = 0.005$; unpaired *t* test; Fig. 1G) or charge (low: 323.1 ± 46.1 fC, $n = 19$; high: 197.8 ± 25.0 fC, $n = 20$; $p = 0.02$; unpaired *t* test). Additionally, we found that EPSCs had faster rise times (low: 0.67 ± 0.05 ms, $n = 19$; high: 0.87 ± 0.08 ms, $n = 21$; $p = 0.046$; unpaired *t* test) and decay times (low: 3.4 ± 0.3 ms, $n = 19$; high: 4.2 ± 0.3 ms, $n = 19$; $p = 0.04$; unpaired *t* test) in low EAAT4 regions (Fig. 1G). Since the number of receptors activated and their binding rate are proportional to agonist concentration (Patneau and Mayer, 1991), the larger EPSC amplitude and faster kinetics suggest a greater [glutamate] reaches MLIs in low EAAT4 regions.

These data are consistent with the idea that EAAT4 expression level regulates extrasynaptic [glutamate], but an alternative explanation is that there are differences in AMPAR density between microzones. To address this possibility, we recorded CF-MLI EPSCs at -60 mV and 40 mV and isolated the NMDAR-mediated EPSCs by applying the NMDAR
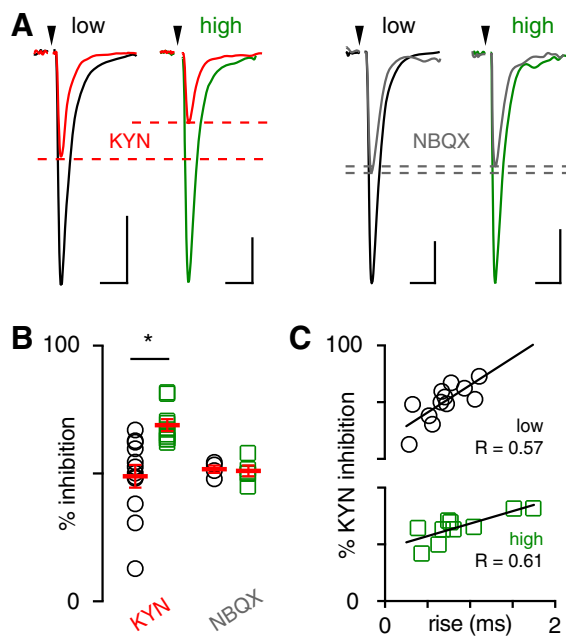
Figure 3. Lower glutamate concentrations mediate spillover EPSCs in high EAAT4 regions. *A*, Representative traces of inhibition of spillover EPSCs by KYN (250 µM, left) and NBQX (100 nM, right) in low and high EAAT4-expressing regions. Scale bars: 20 pA, 10 ms. *B*, EPSCs in high EAAT4 regions were more sensitive to KYN consistent with a lower glutamate concentration (low: 49.8 ± 4.8%, $n = 12$; high: 69.0 ± 2.3%, $n = 10$; $p = 0.003$; unpaired t test). NBQX inhibited EPSC equally in either region (low: 51.7 ± 2.8%, $n = 4$; high: 51.0 ± 4.1%, $n = 0.8$; $p > 0.05$; unpaired t test). *C*, Correlation between KYN inhibition and EPSC rise time in low (black circles) and high (green squares) Venus regions.
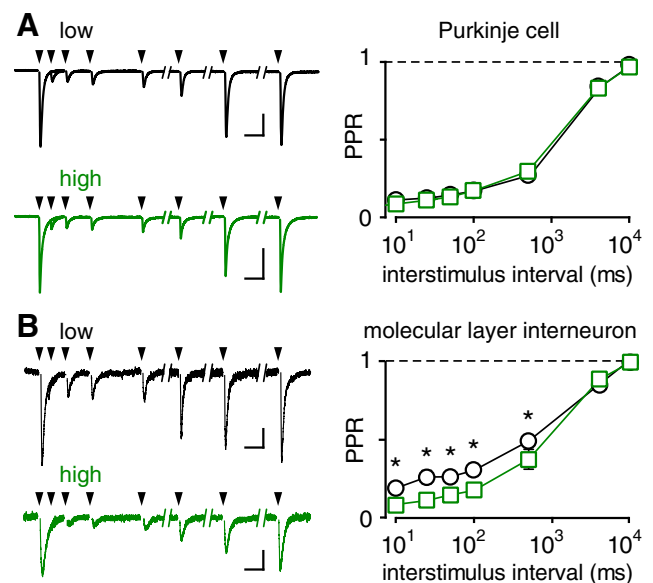

Figure 4. EPSC PPR suggests that spillover differences are not because of presynaptic glutamate release. *A*, Left, Representative EPSCs from PCs in response to paired CF stimuli given at 10, 25, 50, 100, 500 ms, 4 and 10 s apart in low and high EAAT4 regions. Calibration: 500 pA, 20 ms. Right, No difference in PPR at CF-PC synapses in low and high EAAT4 regions ($p > 0.05$ for all time points; $n = 3$ each). *B*, Left, Representative spillover EPSCs from MLIs in response to paired CF stimuli given at 10, 25, 50, 100, 500 ms, 4 and 10 s apart in low and high EAAT4 regions. Calibration: 20 pA, 20 ms. Right, MLIs: $n = 6$ and $n = 5$ (low and high). Multiple unpaired t tests with Holm-Sidak correction ($p = 0.045$, 0.0043, 0.023, 0.012, 0.023, 0.69, and 0.69, respectively).

antagonist R-CPP (5 µM) and subtracting the CPP trace from the control trace (Fig. 2A,B). Similar to AMPAR-mediated EPSCs, the amplitude of the NMDAR-mediated response was significantly larger in low EAAT4 regions than in high EAAT4 regions (low: 29.1 ± 6.7 pA, $n = 6$; high: 5.6 ± 0.7 pA, $n = 5$; $p = 0.01$; unpaired t test; Fig. 2A, right). When we normalized the NMDAR current to the AMPAR-mediated current at −60 mV, there was no difference in the NMDA/AMPA ratio between high and low EAAT4 regions (low: $n = 7$; high: $n = 6$; $p > 0.05$; unpaired t test; Fig. 2B, right). Together, these results argue that differences in receptor expression are not responsible for the distinct spillover responses recorded in high- and low-expressing EAAT4 regions, with the unlikely caveat that the expression of both receptor subtypes is similarly regulated.

To further test the idea that differences in [glutamate] between regions underlie the differences in EPSC properties, we compared the sensitivity of CF-MLI EPSCs to the low-affinity AMPAR antagonist KYN. Unlike high-affinity antagonists (i.e., NBQX) that have a slow unbinding rate, KYN unbinds AMPARs quickly and can be replaced by endogenous glutamate. Thus, inhibition by KYN depends on the [glutamate] and is more effective when the [glutamate] is low. Application of KYN (250 µM) differentially blocked spillover transmission across EAAT4 microzones, reducing the EPSC by 49.8 ± 4.8% ($n = 12$) in low EAAT4 regions and 69.0 ± 2.3% in high EAAT4 regions ($n = 10$; $p = 0.003$; unpaired t test; Fig. 3A,B). As a control, we found that a sub-saturating concentration of the high-affinity antagonist NBQX (100 nM) equally inhibited EPSCs in both regions (low: 51.7 ± 2.8%, $n = 4$; high: 51.0 ± 4.1%, $n = 5$; $p > 0.05$; unpaired t test; Fig. 3A,B). We were surprised there was no correlation

between the % KYN inhibition and the EPSC amplitude (data not shown), suggesting that the amplitude depends not only on the [glutamate] but also the number of available receptors and other factors, such as desensitization. Thus, we turned to a more sensitive measure of [glutamate], the rise time (Coddington et al., 2013). The spillover EPSC rise time is likely more sensitive than the peak amplitude because it less dependent on the number of receptors available to bind glutamate. Indeed, there was a significant correlation between the % KYN inhibition versus rise time for low and high Venus recordings (Fig. 3C). These data support the idea that the rise time of spillover EPSCs reflects the underlying [glutamate] rather than postsynaptic properties, such as receptor density: slower-rising EPSCs are more sensitive to KYN inhibition in both low and high Venus recordings.

Differences in EPSC amplitude are not because of differences in release probability
Our results suggest that spillover EPSCs in high EAAT4 regions are smaller than EPSCs in low EAAT4 regions because of a lower [glutamate] transient. Differences in [glutamate] could result from differences in CF release properties between microzones (Paukert et al., 2010). To test a potential contribution of presynaptic release properties, we compared the paired-pulse ratio (PPR) in low and high EAAT4 regions. The PPR is commonly used to assay release probability (P_r), which together with the size of the readily releasable pool, dictates the extent of multivesicular release and the synaptic [glutamate] (Rudolph et al., 2011; Vaden et al., 2019). We first recorded from PCs, the primary target of CFs, with paired stimuli at various interstimulus intervals (10 ms to 10 s). Recordings were performed in KYN (250 µM) to reduce receptor saturation, leading to a low PPR that recovered

within 10 s, as expected for depletion and recovery of released vesicles (Foster et al., 2002). There was no difference in PPR between high- or low-expressing EAAT4 regions at any interstimulus interval (Fig. 4A; $p > 0.05$), suggesting that differences in presynaptic properties of CFs do not account for the differences in spillover between the two regions. However, since even low levels of receptor saturation might confound precise measurement of PPRs, we repeated the experiment in MLIs with the idea that the low [glutamate] underlying spillover will assure that receptors are far from saturation. Using this assay, we found a slight but significantly greater paired-pulse depression in high EAAT4 regions (Fig. 4B), consistent with lower P_r reported in zebrin-negative zones using other approaches (Paukert et al., 2010). Together, these results confirm that smaller spillover EPSCs in high EAAT4 zones cannot be explained by presynaptic differences since high EAAT4 zones exhibit higher P_r. Our results further argue that high EAAT4 expression is sufficient to limit extrasynaptic glutamate in zebrin-positive zones despite higher P_r at these CF synapses.

Transporter blockers normalize differences in spillover transmission

To directly test whether glutamate uptake capacity underlies differences in glutamate spillover to MLIs, we compared MLI EPSCs in the presence of TBOA (50 μM), an inhibitor of all EAATs. As expected, TBOA significantly increased the EPSC amplitude in both regions (low: from 52.5 ± 15.4 pA to 76.0 ± 17.5 pA, $n = 7$, $p = 0.004$; high: from 20.3 ± 4.2 pA to 56.7 ± 9.4 pA, $n = 8$, $p = 0.0004$; paired t test; Fig. 5A,B). Importantly, the effect of TBOA was more pronounced in high EAAT4 regions (increased by $296 \pm 8\%$ vs $160 \pm 9\%$, $n = 8$, $n = 7$; $p = 0.0005$; Fig. 5C), and there was no difference in EPSC amplitude between low and high EAAT4 regions when EAATs were inhibited (low: 76.0 ± 17.5 pA, $n = 7$; high: 56.7 ± 9.4 pA, $n = 8$; $p > 0.05$; unpaired t test; Fig. 5D). Since the expression levels of glial transporters are similar across the cerebellum (Dehnes et al., 1998), these results suggest that differences in EAAT4 are responsible for differences in EPSC amplitude. To test whether EAAT inhibition also normalized the glutamate transients underlying spillover EPSCs, we compared the sensitivity of CF-MLI EPSCs in the presence of TBOA to KYN, and NBQX. Indeed, there were no differences in KYN or NBQX inhibition between low and high EAAT4 regions in the presence of TBOA (KYN in TBOA low: $53.8 \pm 5.8\%$, $n = 6$; high: $65.2 \pm 6.1\%$, $n = 6$; $p > 0.05$; NBQX in TBOA low: $57.0 \pm 2.2\%$, $n = 5$; high: $53.8 \pm 3.0\%$, $n = 7$; $p > 0.05$; Fig. 5E). Thus, TBOA normalized both the spillover EPSC amplitude and the underlying extrasynaptic [glutamate] between high and low EAAT4 microzones.

Discussion

The stereotyped cytoarchitecture of the cerebellum contrasts with the molecular patterning of gene expression, exemplified by zebrin bands and expression of EAAT4, that represents distinct microzones. Here we show new functional consequences resulting from the differential expression of EAAT4 across microzones that corroborate its rate-limiting role in extrasynaptic glutamate signaling. We visualized the parasagittal banding pattern using Aldoc-Venus mice, showing that Venus correlates with EAAT4 expression. We found that CF-mediated spillover EPSCs to MLIs are smaller in high EAAT4 zones compared with low EAAT4 zones. This difference is explained by the relative [glutamate] reaching receptors on
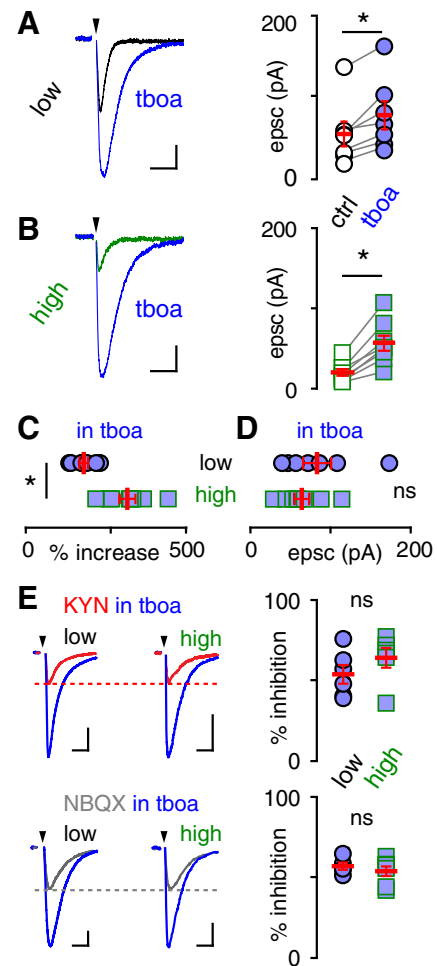

Figure 5. Transporter blockers normalize differences in spillover amplitude in low and high EAAT4 regions. The glutamate transporter antagonist TBOA (blue, 50 μM) increased spillover EPSC amplitudes in both (**A**) low (from 52.5 ± 15.4 pA to 76.0 ± 17.5 pA, $n = 7$, $p = 0.004$; paired t test; calibration: 20 pA, 20 ms) and (**B**) high EAAT4 regions (from 20.3 ± 4.2 to 56.7 ± 9.4, $n = 8$, $p = 0.0004$; paired t test; calibration: 10 pA, 20 ms). **C**, There was a larger increase in EPSC amplitude in high EAAT4 regions (low: $160.1 \pm 8.5\%$, $n = 7$; high: $296.1 \pm 8.4\%$, $n = 8$; $p = 0.0005$) such that (**D**) there was no difference between regions in the presence of TBOA (low: 76.0 ± 23.0 pA, $n = 7$; high: 56.7 ± 16.6 pA, $n = 8$; $p > 0.05$; unpaired t test). **E**, Inhibition of spillover EPSCs by KYN (250 μM, top left; calibration: 20 pA, 20 ms) or NBQX (100 nM, bottom left; calibrations: low, 40 pA, 20 ms; high, 20 pA, 20 ms) in low and high EAAT4 regions in the presence of TBOA (50 μM). EPSCs in high EAAT4 regions were more sensitive to KYN (low: $52.0 \pm 5.6\%$, $n = 5$; high: $71.5 \pm 3.3\%$, $n = 6$; $p = 0.01$), but this difference was normalized in the presence of TBOA (low: $53.8 \pm 5.8\%$, $n = 6$; high: $65.2 \pm 6.1\%$, $n = 6$; $p > 0.05$; top right). There was no difference in inhibition when NBQX was used as a control without TBOA (low: $51.7 \pm 1.4\%$, $n = 4$; high: $51.0 \pm 2.1\%$, $n = 5$; $p > 0.05$) and with TBOA (low: $57.0 \pm 2.2\%$, $n = 5$; high: $53.8 \pm 3.0\%$, $n = 7$; $p > 0.05$; bottom right).

MLIs rather than differences in postsynaptic receptor density or presynaptic release properties. Indeed, despite evidence that CFs in high EAAT4 zones have higher release probability and greater multivesicular release (Paukert et al., 2010), spillover EPSCs were smaller in MLIs from high EAAT4 regions. As both the spillover EPSC and [glutamate] are normalized by EAAT inhibition, together these results indicate that EAAT4 levels are rate-limiting for controlling extrasynaptic glutamate signaling from CFs in the cerebellar cortex.

Regulation of synaptic transmission by EAATs

EAAT4 is one of five isoforms of sodium-dependent glutamate transporters with the primary function of maintaining low extracellular glutamate concentration throughout the CNS (Tzingounis and Wadiche, 2007). EAAT1 and EAAT2, located on glial cells, are responsible for the reuptake of the majority of the glutamate and prevent glutamate excitotoxicity (Rothstein et al., 1994; Tanaka et al., 1997; Danbolt, 2001; Huang et al., 2004, 2005). EAAT3, EAAT4, and EAAT5 are neuronal glutamate transporters responsible for additional functions along with contributing to maintaining low levels of extracellular glutamate (Brasnjo and Otis, 2001; Veruki et al., 2006; Scimemi et al., 2009). Additionally, EAAT3 is proposed to transport glutamate into GABAergic neurons for GABA synthesis (Sepkuty et al., 2002; Mathews and Diamond, 2003). While transporters can have subtle effects on the [glutamate] at synaptic receptors by rapid buffering (Diamond and Jahr, 1997), extensive evidence suggests that transporters primarily control the spread of transmitter outside and between synapses (Tzingounis and Wadiche, 2007). This explains why transport blockers typically have minimal effects on synaptic currents (Hestrin et al., 1990; Sarantis et al., 1993), or peak synaptic [glutamate] (Wadiche and Jahr, 2001), yet can profoundly alter the properties of compound synaptic currents evoked by simultaneous activation of multiple synapses or synaptic currents at specialized synapses (Isaacson and Nicoll, 1993; Asztely et al., 1997; Arnth-Jensen et al., 2002; Bagnall et al., 2011). Indeed, the contribution of extrasynaptic (or "spillover") signaling to direct point-to-point transmission at both glutamatergic and GABAergic synapses can be assessed by the relative sensitivity to inhibition of respective transmitter transporters (Isaacson et al., 1993; Scanziani et al., 1997; Overstreet and Westbrook, 2003; Coddington et al., 2013, 2014; Nietz et al., 2017).

It is generally recognized that the majority of glutamate clearance is mediated by diffusion to glial transporters, but our results point to an important role of neuronal EAAT4 in controlling extrasynaptic glutamate signaling at cerebellar synapses. It has been estimated that as much as 20% of the glutamate released from CFs may be taken up by EAAT4 (Otis et al., 1997) curtailing the PC EPSC duration (Takahashi et al., 1996). EAAT4 is unique in that it is a high-affinity neuronal transporter (10-fold higher than GLAST, GLT, and EAAC) (Arriza et al., 1994; Fairman et al., 1995) present exclusively on PCs (Dehnes et al., 1998; Takayasu et al., 2005). Its postsynaptic localization just outside of CF and PF synapses predicts that even subtle differences in its expression level could influence extrasynaptic glutamate signaling (Dehnes et al., 1998; Zheng et al., 2008). Accordingly, the patterned expression of EAAT4 significantly influences the extent of perisynaptic mGluR activation by glutamate released at PF synapses, as well as activation of AMPARs on adjacent Bergmann glia (Wadiche and Jahr, 2005; Tsai et al., 2012). Since EAAT4 influences signaling to glial cell processes that ensheath PF synapses, we reasoned that EAAT4 may also control extrasynaptic signaling to MLIs that respond to glutamate spillover from CF-PC synapses (Szapiro and Barbour, 2007; Coddington et al., 2013). Indeed, we found that a greater [glutamate] reaches MLIs in low EAAT4 zones than in high EAAT4 zones. When ruling out potential presynaptic differences in glutamate release, we found that CFs in high EAAT4 regions may release more glutamate than CFs in low EAAT4 regions. Despite greater release of glutamate from CFs in zebrin-positive (high EAAT4) zones via multivesicular release (Paukert et al., 2010), a lower [glutamate] reaches glutamate receptors on MLIs.

NMDARs and AMPARs on MLIs are differentially distributed at extrasynaptic and synaptic locations, respectively (Clark and Cull-Candy, 2002). Our results showing NMDAR activation by single CF stimuli are thus consistent with extrasynaptic NMDAR localization. The constant AMPAR/NMDAR ratio across zebrin zones is potentially surprising, considering that higher-affinity NMDARs would be expected to operate within a different region of the glutamate dose–response relationship. However, it is likely that NMDARs and AMPARs are not exposed to the same [glutamate], making it difficult to predict their relative responses. Furthermore, extrasynaptic levels of glutamate resulting from spillover are sub-saturating for both receptor subtypes (Dzubay and Jahr, 1999). Additional studies will be required to identify the precise location of MLI receptors activated by CF spillover, as well as quantify the underlying [glutamate] transient at each receptor subtype.

Implications for MLI function and feedforward inhibition

Zebrin microzones comprise anatomically distinct olivocerebellar modules, with PCs in each zone exhibiting specific input and output projections with the inferior olive and cerebellar nuclei, respectively (Sugihara and Quy, 2007; Ruigrok, 2011). Distinct connectivity and computational power likely underlie distinct cerebellar functions, as zebrin-positive modules in the vestibular cerebellum contribute to adaptation of compensatory eye movements, whereas learning during eyeblink conditioning is associated with zebrin-negative modules (Mostofi et al., 2010; Zhou et al., 2014). Furthermore, it was recently shown that PCs in zebrin-positive zones exhibit relatively lower simple spike firing rates than in zebrin-negative zones, in part because of differential activity of transient receptor potential cation channel C3 (TRPC3), since genetic manipulation of TRPC3 selectively alters the firing rate and behavior associated with zebrin-negative zones (Zhou et al., 2014; Wu et al., 2019). Both LTD of PF inputs and feedforward inhibition by MLIs contribute to PC simple spike suppression during Pavlovian eyeblink conditioning (Boele et al., 2018). EAAT4 expression that can regulate both of these processes (see below) may thus regulate cerebellar plasticity in a microzone-specific fashion and play a role in associative and motor learning. Understanding how the molecular diversity of PCs contributes to distinct cellular functionality may provide insight into specialization of modules that mediate heterogeneous network function.

How might EAAT4 contribute to specialization of cerebellar modules? EAAT4 controls the extent of extrasynaptic glutamate signaling, a function previously shown to regulate synaptic plasticity and simple spiking. In low EAAT4 microzones, glutamate released from PFs can overwhelm local transport capacity to activate perisomatic mGluRs, whereas under the same conditions mGluR activation is absent in high EAAT4 zones (Wadiche and Jahr, 2005). There are multiple consequences of mGluR activation, including a depolarizing conductance mediated by TRPC3, endocannabinoid production that can cause presynaptic inhibition, and induction of LTD of PF synaptic transmission (Kim et al., 2003; Brenowitz and Regehr, 2005). Indeed, low EAAT4 zones exhibit robust LTD of PF synaptic transmission that is absent in high EAAT4 regions (Wadiche and Jahr, 2005). EAAT4-mediated control of extrasynaptic mGluR and NMDAR activation is also associated with differential rates of PC simple spiking (Perkins et al., 2018). Thus, EAAT4 expression plays a cell-autonomous role in PC plasticity and spiking.

In addition to the cell-autonomous function, our new data suggest that EAAT4 regulates activation of glutamate

receptors on MLIs. CFs do not appear to form anatomically defined synapses with MLIs, but glutamate release from CFs activates AMPARs and NMDARs via spillover (Coddington et al., 2013, 2014). Glutamate spillover from a single CF is sufficient to generate both feedforward inhibition and disinhibition of neighboring PCs, with PCs near the active CF receiving a biphasic sequence of inhibition/disinhibition whereas distant PCs exhibit solely disinhibition (Mathews et al., 2012; Coddington et al., 2013). The ability of CFs to excite and inhibit MLIs depends on the proximity of MLIs to CFs, and may explain the response of MLIs to sensory stimulation (Arlt and Hausser, 2020). Regulation of CF spillover to MLIs by EAAT4 expression suggests an additional layer of organization wherein the functionality of these motifs differs across microzones.

References

Arlt C, Hausser M (2020) Microcircuit rules governing impact of single interneurons on Purkinje cell output in vivo. Cell Rep 30:3020–3035.e3023.

Arnth-Jensen N, Jabaudon D, Scanziani M (2002) Cooperation between independent hippocampal synapses is controlled by glutamate uptake. Nat Neurosci 5:325–331.

Arriza JL, Fairman WA, Wadiche JI, Murdoch GH, Kavanaugh MP, Amara SG (1994) Functional comparisons of three glutamate transporter subtypes cloned from human motor cortex. J Neurosci 14:5559–5569.

Asztely F, Erdemli G, Kullmann D (1997) Extrasynaptic glutamate spillover in the hippocampus: dependence on temperature and the role of active glutamate uptake. Neuron 18:281–293.

Bagnall MW, Hull C, Bushong EA, Ellisman MH, Scanziani M (2011) Multiple clusters of release sites formed by individual thalamic afferents onto cortical interneurons ensure reliable transmission. Neuron 71:180–194.

Boele HJ, Peter S, Ten Brinke MM, Verdonschot L, IJpelaar AC, Rizopoulos D, Gao Z, Koekkoek SK, De Zeeuw CI (2018) Impact of parallel fiber to Purkinje cell long-term depression is unmasked in absence of inhibitory input. Sci Adv 4:eaas9426.

Brasnjo G, Otis T (2001) Neuronal glutamate transporters control activation of postsynaptic metabotropic glutamate receptors and influence cerebellar long-term depression. Neuron 31:607–616.

Brasnjo G, Otis T (2004) Isolation of glutamate transport-coupled charge flux and estimation of glutamate uptake at the climbing fiber-Purkinje cell synapse. Proc Natl Acad Sci USA 101:6273–6278.

Brenowitz SD, Regehr WG (2005) Associative short-term synaptic plasticity mediated by endocannabinoids. Neuron 45:419–431.

Chalifoux JR, Carter AG (2011) Glutamate spillover promotes the generation of NMDA spikes. J Neurosci 31:16435–16446.

Clark B, Cull-Candy S (2002) Activity-dependent recruitment of extrasynaptic NMDA receptor activation at an AMPA receptor-only synapse. J Neurosci 22:4428–4436.

Coddington LT, Rudolph S, Vande Lune P, Overstreet-Wadiche L, Wadiche JI (2013) Spillover-mediated feedforward inhibition functionally segregates interneuron activity. Neuron 78:1050–1062.

Coddington LT, Nietz AK, Wadiche JI (2014) The contribution of extrasynaptic signaling to cerebellar information processing. Cerebellum 13:513–520.

Danbolt N (2001) Glutamate uptake. Prog Neurobiol 65:1–105.

Dehnes Y, Chaudhry F, Ullensvang K, Lehre K, Storm-Mathisen J, Danbolt N (1998) The glutamate transporter EAAT4 in rat cerebellar Purkinje cells: a glutamate-gated chloride channel concentrated near the synapse in parts of the dendritic membrane facing astroglia. J Neurosci 18:3606–3619.

Diamond J, Jahr C (1997) Transporters buffer synaptically released glutamate on a submillisecond time scale. J Neurosci 17:4672–4687.

Dzubay J, Jahr C (1999) The concentration of synaptically released glutamate outside of the climbing fiber-Purkinje cell synaptic cleft. J Neurosci 19:5265–5274.

Fairman W, Vandenberg R, Arriza J, Kavanaugh M, Amara S (1995) An excitatory amino-acid transporter with properties of a ligand-gated chloride channel. Nature 375:599–603.

Foster K, Kreitzer A, Regehr W (2002) Interaction of postsynaptic receptor saturation with presynaptic mechanisms produces a reliable synapse. Neuron 36:1115–1126.

Fujita H, Aoki H, Ajioka I, Yamazaki M, Abe M, Oh-Nishi A, Sakimura K, Sugihara I (2014) Detailed expression pattern of aldolase C (Aldoc) in the cerebellum, retina and other areas of the CNS studied in Aldoc-Venus knock-in mice. PLoS One 9:e86679.

Henneberger C, Bard L, Panatier A, Reynolds JP, Kopach O, Medvedev NI, Minge D, Herde MK, Anders S, Kraev I, Heller JP, Rama S, Zheng K, Jensen TP, Sanchez-Romero I, Jackson CJ, Janovjak H, Ottersen OP, Nagelhus EA, Oliet SH, et al. (2020) LTP induction boosts glutamate spillover by driving withdrawal of perisynaptic astroglia. Neuron 108:919–936.e11.

Hestrin S, Sah P, Nicoll RA (1990) Mechanisms generating the time course of dual component excitatory synaptic currents recorded in hippocampal slices. Neuron 5:247–253.

Huang YH, Bergles DE (2004) Glutamate transporters bring competition to the synapse. Curr Opin Neurobiol 14:346–352.

Huang YH, Sinha SR, Tanaka K, Rothstein JD, Bergles DE (2004) Astrocyte glutamate transporters regulate metabotropic glutamate receptor-mediated excitation of hippocampal interneurons. J Neurosci 24:4551–4559.

Huang YH, Sinha SR, Fedoryak OD, Ellis-Davies GC, Bergles DE (2005) Synthesis and characterization of 4-methoxy-7-nitroindolinyl-D-aspartate, a caged compound for selective activation of glutamate transporters and N-methyl-D-aspartate receptors in brain tissue. Biochemistry 44:3316–3326.

Isaacson J, Nicoll R (1993) The uptake inhibitor L-trans-PDC enhances responses to glutamate but fails to alter the kinetics of excitatory synaptic currents in the hippocampus. J Neurophysiol 70:2187–2191.

Isaacson J (1999) Glutamate spillover mediates excitatory transmission in the rat olfactory bulb. Neuron 23:377–384.

Isaacson J, Solís J, Nicoll R (1993) Local and diffuse synaptic actions of GABA in the hippocampus. Neuron 10:165–175.

Jörntell H, Ekerot CF (2002) Reciprocal bidirectional plasticity of parallel fiber receptive fields in cerebellar Purkinje cells and their afferent interneurons. Neuron 34:797–806.

Jörntell H, Ekerot CF (2003) Receptive field plasticity profoundly alters the cutaneous parallel fiber synaptic input to cerebellar interneurons in vivo. J Neurosci 23:9620–9631.

Kim S, Kim Y, Yuan J, Petralia R, Worley P, Linden D (2003) Activation of the TRPC1 cation channel by metabotropic glutamate receptor mGluR1. Nature 426:285–291.

Kollo M, Holderith NB, Nusser Z (2006) Novel subcellular distribution pattern of A-type K^+ channels on neuronal surface. J Neurosci 26:2684–2691.

Kullmann DM (2000) Spillover and synaptic cross talk mediated by glutamate and GABA in the mammalian brain. Prog Brain Res 125:339–351.

Luo Y, Onozato T, Wu X, Sasamura K, Sakimura K, Sugihara I (2020) Dense projection of Stilling's nucleus spinocerebellar axons that convey tail proprioception to the midline area in lobule VIII of the mouse cerebellum. Brain Struct Funct 225:621–638.

Mathews G, Diamond J (2003) Neuronal glutamate uptake contributes to GABA synthesis and inhibitory synaptic strength. J Neurosci 23:2040–2048.

Mathews PJ, Lee KH, Peng Z, Houser CR, Otis TS (2012) Effects of climbing fiber driven inhibition on Purkinje neuron spiking. J Neurosci 32:17988–17997.

Mostofi A, Holtzman T, Grout AS, Yeo CH, Edgley SA (2010) Electrophysiological localization of eyeblink-related microzones in rabbit cerebellar cortex. J Neurosci 30:8920–8934.

Nietz AK, Vaden JH, Coddington LT, Overstreet-Wadiche L, Wadiche JI (2017) Non-synaptic signaling from cerebellar climbing fibers modulates Golgi cell activity. Elife 6:e29215.

Nishiyama H, Linden DJ (2007) Pure spillover transmission between neurons. Nat Neurosci 10:675–677.

Otis TS, Kavanaugh MP, Jahr CE (1997) Postsynaptic glutamate transport at the climbing fiber-Purkinje cell synapse. Science 277:1515–1518.

Overstreet L, Westbrook G (2003) Synapse density regulates independence at unitary inhibitory synapses. J Neurosci 23:2618–2626.

Palay SL, Chan-Palay V (1974) Cerebellar Cortex: Cytology and Organization (Berlin: Springer).

Patneau DK, Mayer ML (1991) Kinetic analysis of interactions between kainate and AMPA: evidence for activation of a single receptor in mouse hippocampal neurons. Neuron 6:785–798.

Paukert M, Huang YH, Tanaka K, Rothstein JD, Bergles DE (2010) Zones of enhanced glutamate release from climbing fibers in the mammalian cerebellum. J Neurosci 30:7290–7299.

Perkins EM, Clarkson YL, Suminaite D, Lyndon AR, Tanaka K, Rothstein JD, Skehel PA, Wyllie DJ, Jackson M (2018) Loss of cerebellar glutamate transporters EAAT4 and GLAST differentially affects the spontaneous firing pattern and survival of Purkinje cells. Hum Mol Genet 27:2614–2627.

Rothstein J, Martin L, Levey A, Dykes-Hoberg M, Jin L, Wu D, Nash N, Kuncl R (1994) Localization of neuronal and glial glutamate transporters. Neuron 13:713–725.

Rudolph S, Overstreet-Wadiche L, Wadiche JI (2011) Desynchronization of multivesicular release enhances Purkinje cell output. Neuron 70:991–1004.

Ruigrok TJ (2011) Ins and outs of cerebellar modules. Cerebellum 10:464–474.

Sarantis M, Ballerini L, Miller B, Silver R, Edwards M, Attwell D (1993) Glutamate uptake from the synaptic cleft does not shape the decay of the non-NMDA component of the synaptic current. Neuron 11:541–549.

Scanziani M (2000) GABA spillover activates postsynaptic GABA(B) receptors to control rhythmic hippocampal activity. Neuron 25:673–681.

Scanziani M, Malenka RC, Nicoll RA (1996) Role of intercellular interactions in heterosynaptic long-term depression. Nature 380:446–450.

Scanziani M, Salin P, Vogt K, Malenka R, Nicoll R (1997) Use-dependent increases in glutamate concentration activate presynaptic metabotropic glutamate receptors. Nature 385:630–634.

Scimemi A, Tian H, Diamond JS (2009) Neuronal transporters regulate glutamate clearance, NMDA receptor activation, and synaptic plasticity in the hippocampus. J Neurosci 29:14581–14595.

Sepkuty J, Cohen A, Eccles C, Rafiq A, Behar K, Ganel R, Coulter D, Rothstein J (2002) A neuronal glutamate transporter contributes to neurotransmitter GABA synthesis and epilepsy. J Neurosci 22:6372–6379.

Sugihara I, Quy PN (2007) Identification of aldolase C compartments in the mouse cerebellar cortex by olivocerebellar labeling. J Comp Neurol 500:1076–1092.

Szapiro GG, Barbour BB (2007) Multiple climbing fibers signal to molecular layer interneurons exclusively via glutamate spillover. Nat Neurosci 10:735–742.

Takahashi M, Sarantis M, Attwell D (1996) Postsynaptic glutamate uptake in rat cerebellar Purkinje cells. J Physiol 497:523–530.

Takayasu Y, Iino M, Kakegawa W, Maeno H, Watase K, Wada K, Yanagihara D, Miyazaki T, Komine O, Watanabe M, Tanaka K, Ozawa S (2005) Differential roles of glial and neuronal glutamate transporters in Purkinje cell synapses. J Neurosci 25:8788–8793.

Takayasu Y, Iino M, Ozawa S (2004) Roles of glutamate transporters in shaping excitatory synaptic currents in cerebellar Purkinje cells. Eur J Neurosci 19:1285–1295.

Tanaka K, Watase K, Manabe T, Yamada K, Watanabe M, Takahashi K, Iwama H, Nishikawa T, Ichihara N, Kikuchi T, Okuyama S, Kawashima N, Hori S, Takimoto M, Wada K (1997) Epilepsy and exacerbation of brain injury in mice lacking the glutamate transporter GLT-1. Science 276:1699–1702.

Tsai MC, Tanaka K, Overstreet-Wadiche L, Wadiche JI (2012) Neuronal glutamate transporters regulate glial excitatory transmission. J Neurosci 32:1528–1535.

Tsukada S, Iino M, Takayasu Y, Shimamoto K, Ozawa S (2005) Effects of a novel glutamate transporter blocker, (2S, 3S)-3-[3-[4-(trifluoromethyl)benzoylamino]benzyloxy]aspartate (TFB-TBOA), on activities of hippocampal neurons. Neuropharmacology 48:479–491.

Tzingounis AV, Wadiche JI (2007) Glutamate transporters: confining runaway excitation by shaping synaptic transmission. Nat Rev Neurosci 8:935–947.

Vaden JH, Banumurthy G, Gusarevich ES, Overstreet-Wadiche L, Wadiche JI (2019) The readily-releasable pool dynamically regulates multivesicular release. Elife 8:e47434.

Veruki M, Mørkve S, Hartveit E (2006) Activation of a presynaptic glutamate transporter regulates synaptic transmission through electrical signaling. Nat Neurosci 9:1388–1396.

Wadiche JI, Jahr CE (2001) Multivesicular release at climbing fiber-Purkinje cell synapses. Neuron 32:301–313.

Wadiche JI, Jahr CE (2005) Patterned expression of Purkinje cell glutamate transporters controls synaptic plasticity. Nat Neurosci 8:1329–1334.

Wu B, Blot FG, Wong AB, Osório C, Adolfs Y, Pasterkamp RJ, Hartmann J, Becker EB, Boele HJ, De Zeeuw CI, Schonewille M (2019) TRPC3 is a major contributor to functional heterogeneity of cerebellar Purkinje cells. Elife 8:e45590.

Xu-Friedman M, Harris K, Regehr W (2001) Three-dimensional comparison of ultrastructural characteristics at depressing and facilitating synapses onto cerebellar Purkinje cells. J Neurosci 21:6666–6672.

Zheng K, Scimemi A, Rusakov D (2008) Receptor actions of synaptically released glutamate: the role of transporters on the scale from nanometers to microns. Biophys J 95:4584–4596.

Zhou H, Lin Z, Voges K, Ju C, Gao Z, Bosman LW, Ruigrok TJ, Hoebeek FE, De Zeeuw CI, Schonewille M (2014) Cerebellar modules operate at different frequencies. Elife 3:e02536.